

Preparation and Magnetic Properties of Ni/Pd Multilayer Nanowire Arrays

Babak Jaleh · Fatemeh Koosha ·
Afshan Omidvar Dezfuli

Received: 18 July 2013 / Accepted: 13 September 2013 / Published online: 29 September 2013
© Springer Science+Business Media New York 2013

Abstract Ni/Pd multilayer nanowire arrays have been electrodeposited into the nanochannels of porous polycarbonate (PC) template. Current–time profiles obtained during the deposition process were analyzed to understand the mechanism of growth. Synthesized nanowires were fully characterized by X-ray diffraction (XRD), energy dispersive X-ray (EDX), and scanning electron microscopy (SEM). The X-ray diffraction pattern showed that Pd and Ni grow in their face-centered-cubic (FCC) structures. Each nanowire had the same length of $\approx 4 \mu\text{m}$ and a diameter of 90 nm. The magnetic properties of the prepared nanowires are different under different electrodeposition conditions. A vibration sample magnetometer (VSM) was used to determine the effect of the Pd content on magnetic properties of final products.

Keywords Ni/Pd multilayer nanowire · Electrodeposition · Polycarbonate template

1 Introduction

One-dimensional structures such as nanowires, nanorods, nanotubes, and nanobelts exhibit unusual behavior compared to their bulk counterparts; e.g., the manifestation of

quantum phenomena in the electron transport of metallic nanowires, [1] enhancement in the mechanical strength and hardness [2, 3], the interesting magnetic properties including giant magnetic resonance of nanowires [4], and decay of wires into chains of nanospheres stimulated by Rayleigh instability [5, 6]. In particular, nanowires are very suitable for investigating the dependence of physicochemical properties on size reduction and are tipped to play an important role both as interconnects and functional units in future electronic, optoelectronic, electrochemical, sensoric, and electromechanical devices with nanoscale dimensions [7, 8].

Palladium nanowire arrays can be used as hydrogen sensors and hydrogen-actuated switches that exhibit a response time ranging from 20 ms to 5 s, depending on the hydrogen concentration [9]. This hydrogen sensor can potentially exhibit a fast response with a substantially higher sensitivity and selectivity, but palladium can be poisoned easily by exposure to reactive species such as hydrocarbons, O_2 , H_2O , and CO_2 [10]. In addition, pure palladium can produce hydrogen bubbles, which cause the sensors not to work normally [11, 12]. It has been demonstrated in many reports that bimetallic catalysts are more efficient in catalytic reduction as compared to monometallic ones. The bimetallic catalysts consist of a noble metal (Pd, Pt, and Rh) and a promoting transition metal (Cu, Ni, Fe, Sn, and In) [13, 14]. The role of the transition metal is to reduce toxic ions according to a redox process leading to its oxidation; the role of the noble metal is to stabilize the transition metal in its lower oxidation states [15].

Nanowires can be fabricated by diverse techniques including lithographic patterning [16, 17] vapor transport techniques [18–21], template based-synthesis method, laser ablation [22, 23], and other synthesis methods [24–28]. The template-based synthesis involving electrodeposition is more promising owing to its specific advantages of low

B. Jaleh (✉) · A.O. Dezfuli
Physics Department, Bu-Ali Sina University, Hamedan, Iran
e-mail: jaleh@basu.ac.ir

B. Jaleh
e-mail: bkjaleh@yahoo.com

F. Koosha
Department of Physics, Science and Research, Islamic Azad University, Hamedan, Iran

cost and control over the nanowires properties via changing the electrolyte composition, pH, temperature, and applied potential/current [29]. Possin was the first to report the electrodeposition of nanowires using a template-based method [30]. A comprehensive overview of the membrane/template based preparation method for a wide variety of nanowires has been covered in various reviews [31, 32].

In this work, the electrodeposition technique has been used to fill the polycarbonate template pores with Ni/Pd multilayer nanowires since the method is more reliable for deposition into high aspect ratio materials and can compensate for the slow diffusion-driven transport in the narrow pores. XRD and SEM were used to study the crystalline structure and morphologies of the fabricated Ni/Pd multilayer nanowires. The chemical composition of the prepared nanostructures was measured by EDX performed in SEM. Variation in magnetic behavior of the synthesized nanowires, at different deposition times for each sample, was investigated using VSM measurements. Moreover, the VSM results were used for determining the effect of the Pd content on magnetic properties of the final products.

2 Experimental

Commercially available ion track-etched polycarbonate templates with a pore diameter of 100 nm, pore length of 4 μm (Millipore, USA) were used as a template material for growing multilayer nanowires. A gold layer of approximately 100 nm thick was sputtered at the backside of this membrane. The gold-sputtered membrane was used as the working electrode of the electrodeposition process. A small platinum mesh was used as the counter electrode and Ag/AgCl in 3 M KCl was used as the reference electrode. The electrodeposition takes place inside the nanopores, starting from the metal layer. The template was then placed in a custom-built electrochemical cell. A three electrode electrochemical cell was used during this work to electrodeposit Ni/Pd multilayer nanowires at room temperature.

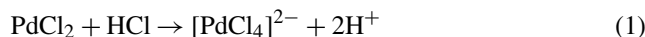
Structure of synthesized nanowires was studied using X-ray diffraction (Philips powder diffractometer type PW 1373 gonimeter). The XRD was equipped with a graphite monochromator crystal. The X-ray wavelength was 1.5405 Å and diffraction patterns were recorded in a 2θ range (0–80°) with a scanning speed of 2°/min. To obtain the SEM images of electrodeposited nanowires, polycarbonate templates were dissolved in dichloromethane and the remains consisted of nanowires and a gold layer were served as a sample for the SEM observation. The sample morphology and images of nanowires were studied by VEGA TES-can SEM. The chemical composition of the prepared nanostructures was measured by EDX performed in the SEM. The

magnetic measurement was carried out in the VSM at room temperature.

3 Results and Discussion

3.1 Fabrication of Multilayer Nanowire Arrays

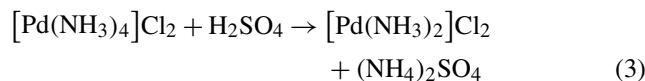
Using the dual-bath technique, Ni and Pd segments were alternately electrodeposited into the pores for the same time by moving the substrate between two different electrolyte baths. One bath consisted of 225 g/l $\text{NiSO}_4 \cdot 6\text{H}_2\text{O}$, 30 g/l $\text{NiCl}_2 \cdot 6\text{H}_2\text{O}$, and 30 g/l H_3BO_3 [7]. The Pd nanowires electrodepositions were carried out in a $\text{Pd}(\text{NH}_3)_2\text{Cl}_2$ solution, prepared according to the following procedure: PdCl_2 was added to hydrochloric acid and stirred until it was completely dissolved, leaving a brown transparent solution.



Pink-colored $\text{Pd}(\text{NH}_3)_2\text{Cl}_2$ appeared when the solution was dropped into diluted ammonia as follows:



The solution was stirred at 70 °C for 1 h. The pH value of the solution was then adjusted to 7 by the addition of diluted sulfuric acid as follows [33]:



The electrochemical behavior of Ni^{2+} and Pd^{2+} on the polycarbonate template was investigated using cyclic voltammetry (Fig. 1). Figure 1 shows that deposition potential of Ni^{2+} and Pd^{2+} on polycarbonate template is +0.5 and –1.00 V, respectively.

The deposition process was accomplished while monitoring the current-time profiles to derive information related to the growth mechanism.

The product of the current and the time determined the deposited amount of Ni and Pd at the cathode. Figure 2 shows current-time diagram during electrodeposition of Ni/Pd multilayer nanowires in polycarbonate template. It includes (a): 10 s electrodeposition of Ni^{2+} ions at –1.1 V and then 200 s for Pd^{2+} ions at –1 V, (b): 10 s electrodeposition of Ni ions at –1.1 V and then 100 s for Pd ions at –1 V, (c): 30 s electrodeposition of Ni ions at –1.1 V and then 100 s for Pd ions at –1 V. Figure 2 shows that cathodic current produced during electrodeposition of Ni layer is more than that of Pd layer. This may be due to the higher concentration and higher applied overvoltage of Cu ions compared with Pd ions. Our purpose is to understand the effect of different deposition times on the structural and magnetic properties of the Ni/Pd multilayer nanowires.

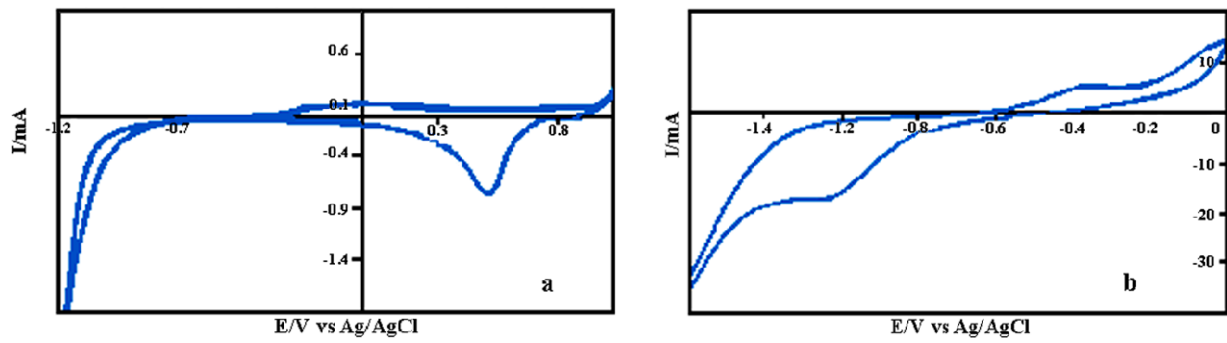


Fig. 1 Cyclic voltammograms of (a) Ni²⁺ and (b) Pd²⁺ ions on polycarbonat template

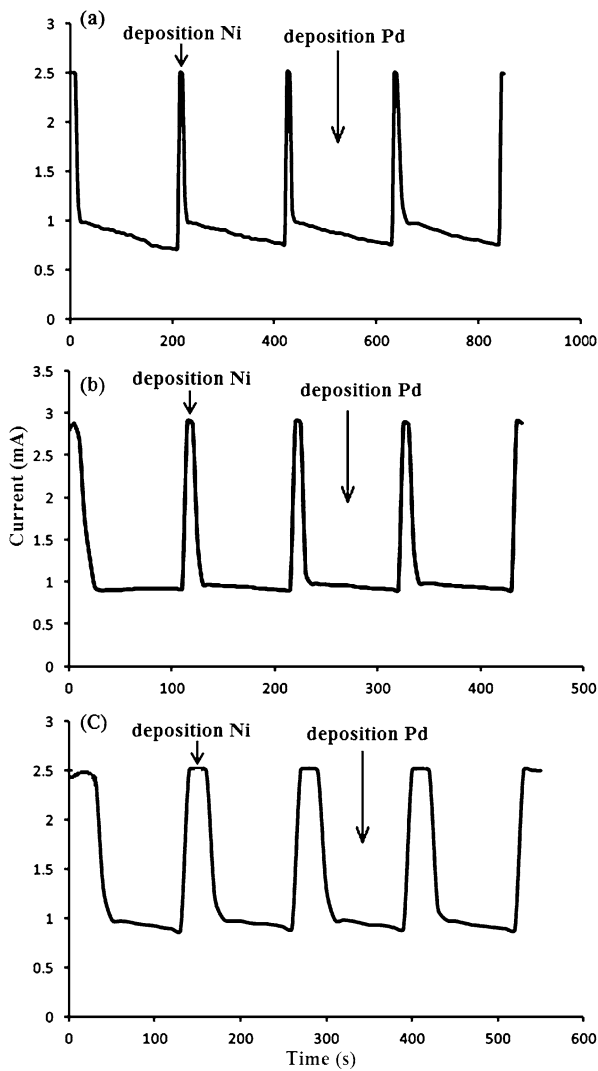


Fig. 2 The current transient during the electrodeposition of the Ni/pd multilayer nanowires in the polycarbonat template. (a): 10 s electrodeposition of Ni ions at -1.1 V and then 200 s for Pd ions at -1 V, (b): 10 s electrodeposition of Ni ions at -1.1 V and then 100 s for Pd ions at -1 V, (c): 30 s electrodeposition of Ni ions at -1.1 V and then 100 s for Pd ions at -1 V

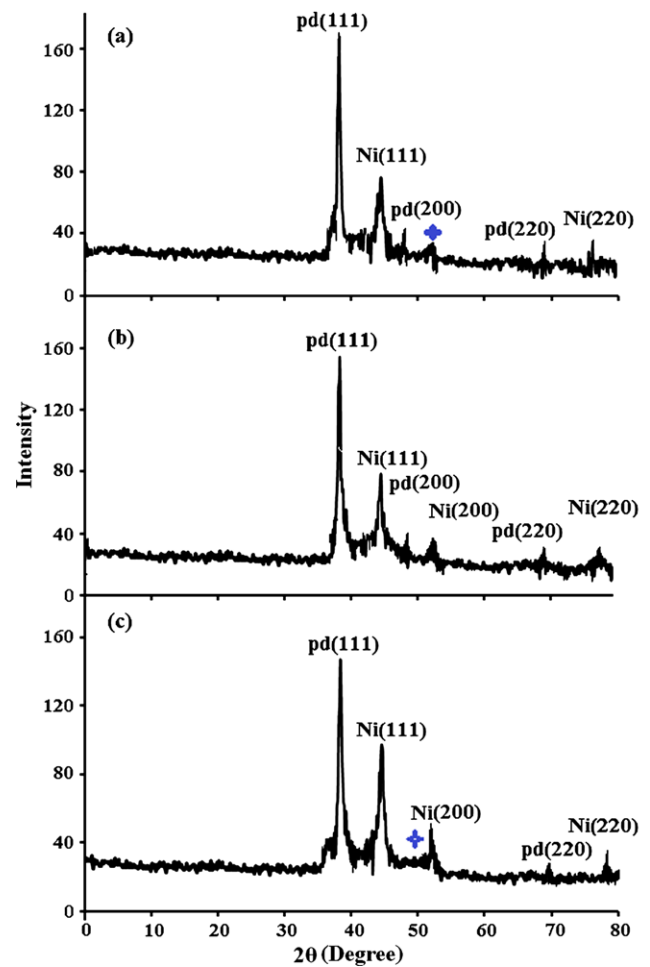
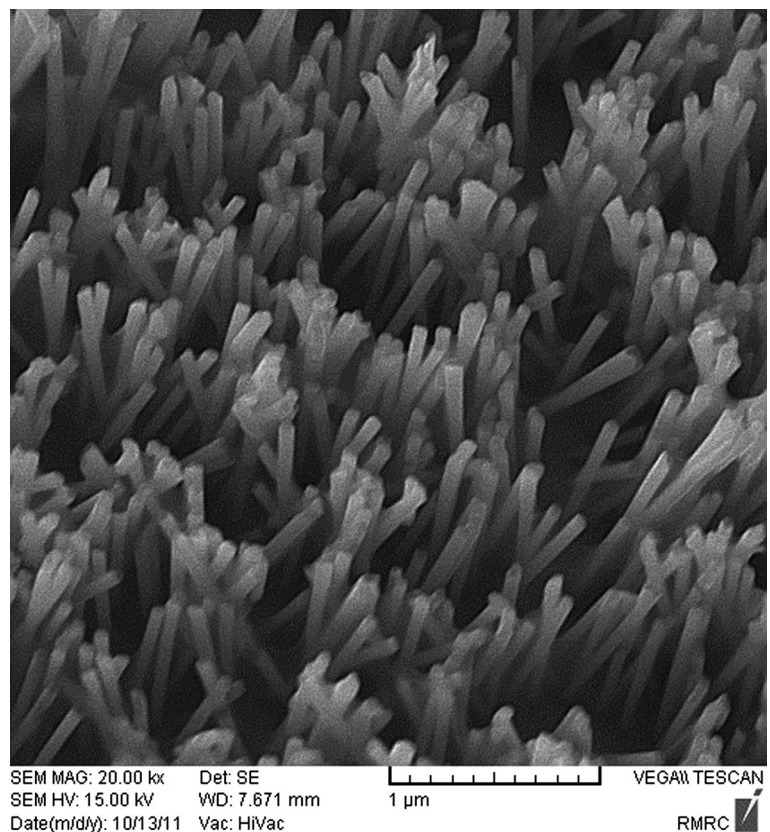


Fig. 3 XRD patterns of the segmented Ni/Pd multilayer nanowires deposited at different times. (a): electrodeposition 10 s of the Ni layer and electrodeposition 200 s of the Pd layer, (b): electrodeposition 10 s of the Ni layer and electrodeposition 100 s of the Pd layer, (c): electrodeposition 30 s of the Ni layer and electrodeposition 100 s of the Pd layer

Fig. 4 Typical SEM image of Ni/Pd multilayer nanowires



3.2 Crystal Structure and Morphology

Structure of the samples was studied using the XRD technique. Figure 3 showed XRD patterns of the segmented Ni/pd multilayer nanowires at different deposition times. The sharp peaks of the (111), (200), (220) diffractions indicate that the Pd and Ni segment has FCC structure [7].

Figure 3 shows that the peaks' intensity of the Ni segment increases and the peaks' intensity of the Pd segment decreases. This is due to the increased time of Ni deposition. The sharp diffraction peaks of the sample indicated that Ni/Pd multilayer nanowires have been well crystallized. No characteristic peaks of other impurities have been detected, indicating the high purity products.

Figure 4 shows the typical SEM image of the Ni/Pd multilayer nanowires electrodeposited in the porous polycarbonate templates. Clearly, the nanowires are cylindrical shape and almost each nanowire has a diameter of 90 nm.

A quantitative EDX spectrum was taken to determine the elemental composition of the Ni/Pd multilayer nanowires. The results are presented in Fig. 5. From this figure, it is confirmed that there are no other elemental impurities present in the nanowires composition. This analysis gives the percent by weight (wt %) and percent number of atoms (at %) of each elemental identified (Table 1).

Figure 6(a–c) shows the magnetic hysteresis loops of Ni/Pd multilayer nanowires at different deposition times at

room temperature. The measurements were performed with the magnetic field applied perpendicular to the polycarbonate template plane. The results of M_S and M_R are summarized in Table 2.

As shown in Table 2, the magnetic property of sample “c” is better than that of the other samples because the thickness of the Ni layers is sample “c” more than other samples.

4 Conclusion

The present work describes the successful fabrication of Ni/Pd multilayer nanowires in the PC template by the electrodeposition method. The Ni/Pd multilayer nanowires have the diameters of about 90 nm. The growth mechanism and the behavior of current-time curves are investigated in detail. The proposed explanation of the mechanism enables us to in-situ control of the growth of multilayer nanowires by controlling current-time transients. The fabricated Ni/Pd multilayer nanowires are well arranged. The XRD pattern shows that multilayer nanowires consist of a pure phase of nickel and palladium with FCC structure without a preferred orientation. The magnetic properties of nanowires increased with an increase in the thickness of Ni layers. We believe that such structures can be used as an active element for sensor and catalyst applications.

Fig. 5 EDX of the Ni/Pd multilayer nanowires deposited in polycarbonate template. (a): electrodeposition 10 s of the Ni layer and electrodeposition 200 s of the Pd layer, (b): electrodeposition 10 s of the Ni layer and electrodeposition 100 s of the Pd layer, (c): electrodeposition 30 s of the Ni layer and electrodeposition 100 s of the Pd layer

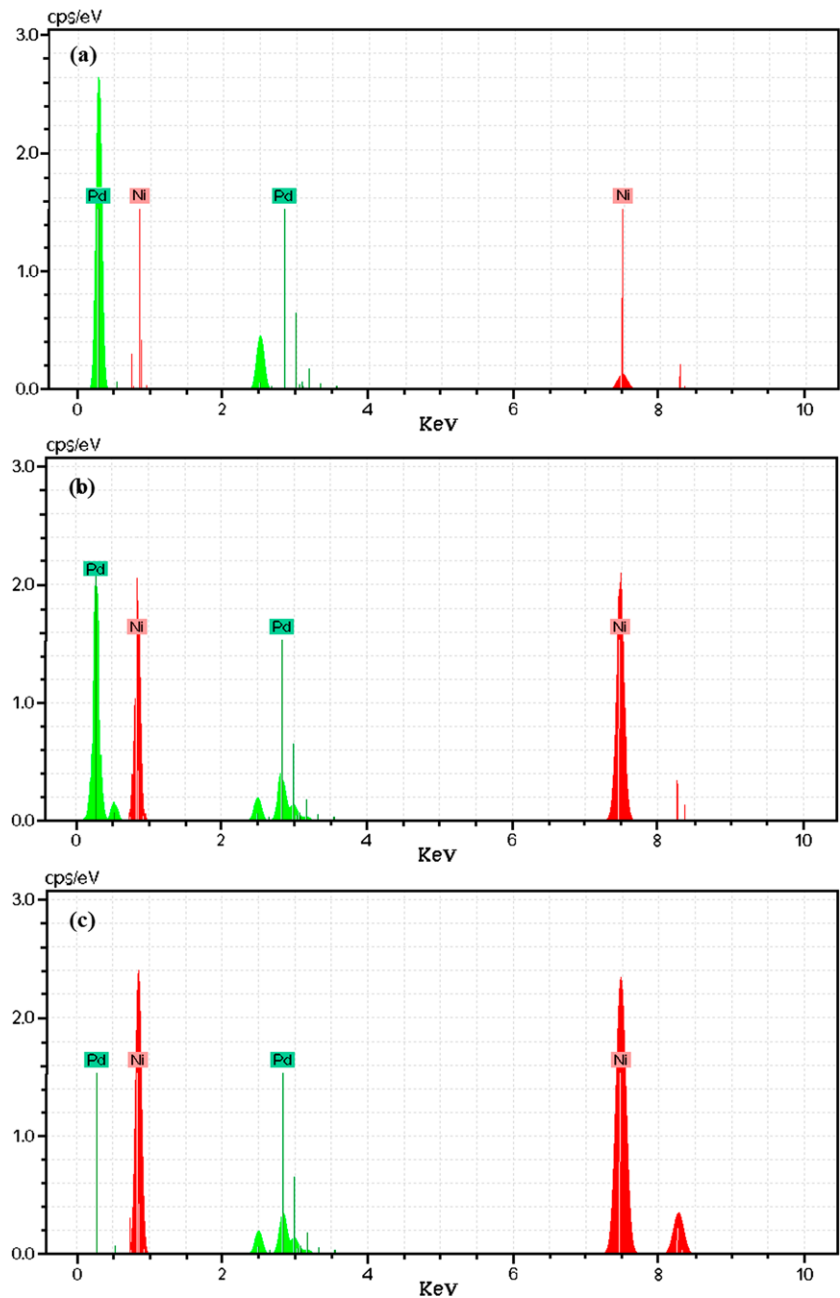


Table 1 EDX elemental analysis of the Ni/Pd multilayer nanowires. (a): electrodeposition 10 s of Ni layer and electrodeposition 200 s of Pd layer, (b): electrodeposition 10 s of Ni layer and electrodeposition 100 s of Pd layer, (c): electrodeposition 30 s of Ni layer and electrodeposition 100 s of Pd layer

Deposition times ratio (Ni/Pd)	Wt%		At%	
	Ni	Pd	Ni	Pd
a: 10 s/200 s	58.38	41.62	71.78	28.22
b: 10 s/100 s	76.1	23.9	84.13	15.87
c: 30 s/100 s	93.82	6.18	96.49	3.51

Table 2 M_S and M_R of Ni/Pd multilayer nanowires (a): electrodeposition 10 s of Ni layer and electrodeposition 200 s of Pd layer, (b): electrodeposition 10 s of Ni layer and electrodeposition 100 s of Pd layer, (c): electrodeposition 30 s of Ni layer and electrodeposition 100 s of Pd layer

Deposition times (Ni/Pd)	M_S	M_R
a: 10 s/200 s	0.00894	0.001525
b: 10 s/100 s	0.007815	0.00237
c: 30 s/100 s	0.007315	0.006385

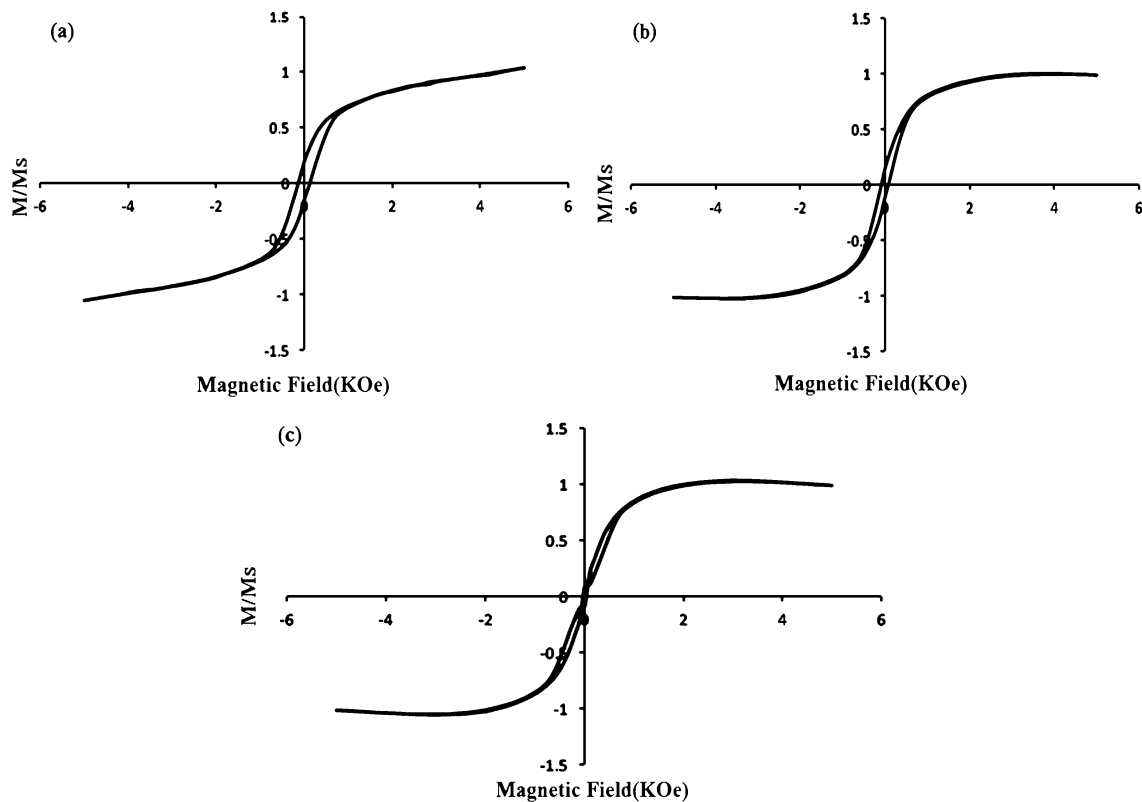


Fig. 6 Hysteresis loops of electrodeposited Ni/Pd multilayer nanowires in parallel directions to the applied magnetic field (a): electrodeposition 10 s of the Ni layer and electrodeposition 200 s of the Pd

layer, (b): electrodeposition 10 s of the Ni layer and electrodeposition 100 s of the Pd layer, (c): electrodeposition 30 s of the Ni layer and electrodeposition 100 s of the Pd layer

References

- Cornelius, T.W., Toimil-Molares, M.E., Karim, S., Neumann, R.: *Phys. Rev. B* **77**, 125425 (2008)
- Jaleh, B., Omidvar Dezfouli, A.: *Solid State Commun.* **166**, 1–86 (2013)
- Wu, B., Heidelberg, A., Boland, J.J., Sader, J.E., Sun, X.-M., Li, Y.D.: *Nano Lett.* **6**, 468 (2005)
- Bouhou, S., Essaoudi, I., Ainane, A., Dujardin, F., Ahuja, R., Saber, M.: *J. Supercond. Nov. Magn.* **26**, 201–211 (2013)
- Karim, S., Toimil-Molares, M.E., Balogh, A.G., Ensinger, W., Cornelius, T.W., Khan, E.U., Neumann, R.: *Nanotechnology* **17**, 5954 (2006)
- Ghaddar, A., Gloaguen, F., Gieraltowski, J., Tannous, C.: *Physica B* **406**, 2046 (2011)
- Jaleh, B., Omidvar-Dezfouli, A., Jaberian-Hamedan, V., Najafi, M., Tamari, E.: *Int. J. Phys. Sci.* **6**, 4775 (2011)
- Kline, T.R., Tian, M., Wang, J., Sen, A., Chan, M.W.H., Mallouk, T.E.: *Inorg. Chem.* **45**, 7555 (2006)
- Walter, E.C., Favier, F., Penner, R.M.: *Anal. Chem.* **74**, 1546 (2002)
- Christofides, C., Mandelis, A.: *J. Appl. Phys.* **68**, R1 (1991)
- Favier, F., Walter, E.C., Zach, M.P., Benter, T., Penner, R.M.: *Science* **293**, 2227 (2001)
- Scharnagl, K., Eriksson, M., Karthigeyan, A., Burgmair, M., Zimmer, M., Eisele, I.: *Sens. Actuators B* **78**, 69–72 (2001)
- Vorlop, K.D., Prusse, U.: In: Jansen, F.J., van Santen, R.A. (eds.) *Catalytic Science Series*, vol. 1 (1999)
- Prusse, U., Vorlop, K.D.: *J. Mol. Catal. A, Chem.* **173**, 313 (2001)
- Jaleh, B., Omidvar Dezfouli, A., Madrakian, T., Ahmadi, M.: *Iran. J. Phys. Res.* **12**, 39–42 (2012)
- Bandaru, P.R., Pichanusakorn, P.: *Semicond. Sci. Technol.* **25**, 024003 (2010)
- Rahman, S.F.A., Hashim, U., Nor, M.N.Md., Mohamed Nuri, A.M., Shohini, M.E.A., Salleh, S.: *AIP Conf. Proc.* **1136**, 504 (2009)
- Malandrino, G., Finocchiaro, S.T., Nigro, R.L., Bongiorno, C., Spinella, C., Fragala, I.L.: *Chem. Mater.* **16**, 5559 (2004)
- Kim, H.W., Kim, N.H.: *Appl. Phys. A, Mater. Sci. Process.* **81**, 763 (2005)
- Suliaman, K.M., Huang, X., Liu, J., Tang, M.: *Smart Mater. Struct.* **16**, 89 (2007)
- Bae, S.Y., Seo, H.W., Park, J.H.: *J. Phys. Chem. B* **108**, 5206 (2004)
- Mehri, A., Seyyed Ebrahimi, S.A., Abdizadeh, H.: *J. Supercond. Nov. Magn.* **25** (2012)
- Kline, T.R., Tian, M., Wang, J., Sen, A., Chan, M.W.H., Mallouk, T.E.: *Inorg. Chem.* **45**, 7555 (2006)
- Xu, C., Xu, G., Liu, Y., Wang, G.: *Solid State Commun.* **122**, 175 (2002)
- Cao, M., Wang, Y., Guo, C., Qi, Y., Hu, C., Wang, E.: *J. Nanosci. Nanotechnol.* **4**, 824 (2004)
- Oates, T.W.H., Keller, A., Noda, S., Facsko, S.: *Appl. Phys. Lett.* **93**, 063106 (2008)
- Chen, Y.W., Liu, Y.C., Lu, S.X., Xu, C.S., Shao, C.L., Wang, C., Zhang, J.Y., Lu, Y.M., Shen, D.Z., Fan, X.W.: *J. Chem. Phys.* **123**, 134701 (2005)

28. Zheng, D., Sun, S., Fan, W., Yu, H., Fan, C., Cao, G., Yin, Z., Song, X.: *J. Phys. Chem. B* **109**, 16439 (2005)
29. Gupta, M., Pinisetty, D., Flake, J.C., Spivey, J.J.: *J. Electrochem. Soc.* **157**, D473 (2010)
30. Possin, G.E.: *Rev. Sci. Instrum.* **41**, 772 (1970)
31. Hulteen, J.C., Martin, C.R.: *J. Mater. Chem.* **7**, 1075 (1997)
32. Chakarvarti, S.K., Vetter, J.: *Radiat. Meas.* **29**, 149 (1998)
33. Tasaltin, N., Ozturk, S., Kilinc, N., Yuzer, H., Ozturk, Z.Z.: *J. Alloys Compd.* **509**, 3667 (2011)